# Optical Fluorescent Measurement Method for the Film Height Determination of Compliant Slider Bearings

A.H. Sahetapy (4588827), M.G.C. de Groot (4463528), R. M. Lingmont (4473248),
W.J.B. Nederstigt (4204344), J.P.A. Nijssen (Supervisor) and R.A.J van Ostayen (Supervisor) PME A-12

***Abstract*— Conventional hydrostatic slider bearings are stiff machine components where, to determine the film height, measuring at one location is usually sufficient. However, for highly flexible sliders for non-planar bearing surfaces this approach does not apply. Possible applications for these kind of bearings include water pumps and lathes where eccentric varying running tracks and running tracks with surface waviness are present. A reliable measurement method to determine the complete bearing surface film height is thus desired.**

**An optic fluorescence based method is presented; fluorescent pigments are dissolved into the water based lubrication medium. Light with a wavelength of 540 $nm$ is cast onto different stationary slider surfaces with predetermined surface waviness. The sliders are suspended in a transparent container filled with the medium. Light scattered from the slider surface and emitted by the fluorescent pigment is captured by a colour camera. The ratio between the red and green channels is proportional to the film height. Resulting images are compared to white light interferometer scans to determine the accuracy of the measurement method. Using this technique, the film thickness can be determined with an accuracy in the order of 10 $\mu m$ over the entire slider surface.**

## I. Introduction

Classic hydrostatic thrust bearings are highly suitable for reliable motion performance; they can operate under high working loads, while causing hardly any friction or wear. However, their applicability is limited by the fact that they require the running track to have constant curvature [1].

Compliant hydrostatic bearings can eliminate this problem. They are unique in their ability to change shape, according to the pressure exerted by its liquid film [2]. Such a design would combine the advantages of hydrostatic bearings with the ability to run on a track of varying curvature or large surface waviness, without loss of performance.

Therefore, they are excellent for use in hydraulic pumps a running track of varying curvature is required [3]. They can also be implemented in lathes, where a running track with surface waviness is present [4].

The performance and wear of hydrostatic bearings depends on the thickness of the lubrication film between the bearing and its track. Contemporary measurement techniques use a single point measurement and assume a rigid bearing surface [5]. However, for compliant hydrostatic bearings this assumption cannot be made as the surface is non-constant and deforms according to the pressure exerted on it by the lubrication film [2].

Thus a new measurement approach needs to be investigated. This new measurement technique must be able to determine the film height of each point on the entire bearing and should lead to the creation of a height map.

Possible existing measurement methods have unsatisfactory precision, such as *laser absorption* [6], but most are not able to take measurements along a surface, including *ultrasound* [7], *light microscopy* [8], *laser absorption* [6] and *internal reflection* [9]. Other methods simply proved too costly or complex to implement, such as *optical interferometry* [10] [11] or *Photogrammetry* [12]. However, methods using *fluorescence* [13][14] or *dye attenuation* [15] have more potential to be adapted, as they both capture an image, which is a 2D measurement. This means that taking one measurement is sufficient. In principle, both methods use colour differences to measure film thickness. As fluorescence is likely to cause a larger colour shift, as will be explained later, it is easier to measure small film thicknesses.

Therefore, this paper will explore the possibility of adapting a fluorescence based measurement technique to perform a distributed film height measurement over the bearing surface.

This design study has been conducted as part of the Bachelor End Project for third year Bachelor Mechanical Engineering students at the TU Delft.

## II. Method

The method described by Husen et al. [13] works on the principle of fluorescence. Fluorescent materials absorb electromagnetic radiation and reemit that radiation at a different wavelength. Fluorescent molecules are excited by a photon which shifts an electron into a higher orbit. When the electron returns to its ground state, a photon is emitted. This electromagnetic radiation usually has a longer wavelength and thus lower energy than the absorbed radiation. This difference causes a shift in colour, called the Stokes shift. The molecules have a specific sensitivity to different wavelengths, creating absorption and emission spectra.

Husen et al. [13] presents a method for measuring the thickness of an oil film using fluorescence; a fluorescent pigment is dissolved in the liquid film and fluorescence is induced by casting light upon it from a LED. Then, both $E_{\lambda_{fl}}$, the intensity of the fluorescent light, and $E_{\lambda_i}$, the intensity of incident light from the LED, are registered using a camera. These wavelengths can either be filtered digitally, using the specific colour sensitivity of the camera, or with the use of optical band-pass filters.

Husen et al. [13] derives the equation for the ratio $R$ between these intensities for each camera pixel as follows:

$$R = \frac{E_{\lambda_{fl}} - D}{E_{\lambda_i} - D} - R_{h=0} \quad (1)$$

Where $D$ is the intensity when no light is present, and $R_{h=0}$ is the ratio at the point where no fluorescent film is present.

This ratio is proportional to the film thickness. Husen et al. [13] introduces a scaling factor $a$ to relate the ratio to the real height 2.

$$h = a \cdot R \quad (2)$$

The major advantage of using this method is that it is independent of time and the angle of the camera and LED up to 70° [13]. This method can be implemented for measuring compliant bearing film height by adjusting some key parameters.

A different pigment has to be used, since for the design applications the preferred lubrication medium is water, which severely limits the amount of suitable pigments. Ultimately, *Rhodamine B* was selected for its relatively good solubility in water of 1 $\frac{g}{L}$ [16] and the coincidence of the emission spectrum with the sensitivity spectra of the camera sensor. In addition, it was already available at the faculty.

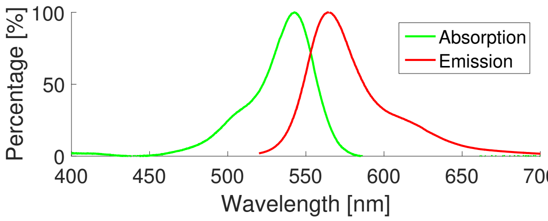


Fig. 1: Rhodamine B emission & absorption spectra in ethanol [17]

The absorption and emission spectra of *Rhodamine B* in ethanol are shown in figure 1. The characteristics of *Rhodamine B* in ethanol are comparable to those in water [18].

A LED was selected so that the emission spectrum of the LED matched the absorption spectrum of *Rhodamine B*. The scaling factor $a$ is originally calculated by Husen et al. [13] using a known volume of liquid to determine the film thickness. This is however not applicable to the development of compliant hydrostatic bearings, as the volume beneath the bearing will be variable when the bearing deforms. Therefore, two measurements with known film thickness are used for calculating the scaling factor $a$.

The method used by Husen et al. [13] is intended for a film with a free surface. In the case of a compliant bearing a solid counter surface will always be present, influencing the measurement. This counter surface thus has to be transparent. The assumption is made that counter surface is a perfectly transparent plate. The surface roughness of the plate is less then 1 $\mu m$ [19] so it is also assumed perfectly smooth and flat. Figure 2 represents a schematic of the test setup.

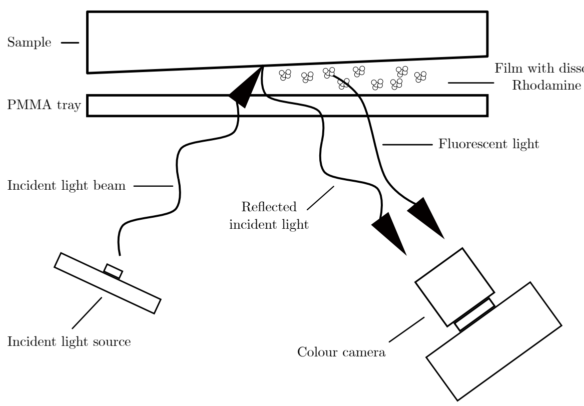


Fig. 2: Schematic of the test setup

## III. Results

### A. Setup

Two different samples are constructed out of a $8 \cdot 5 \cdot 2\ cm$ slab of aluminium. The first sample has slope of 1 $mm$ over the length of its surface, the second sample is slotted with a ball end mill at depths of $0.25,\ 0.30\ and\ 0.50\ mm$. A frame is constructed out of Thorlabs optical rails in order to suspend a PMMA tray over a camera and a LED with a wavelength between $535 - 545\ nm$. The tray is filled with *Rhodamine B* dissolved in water at a concentration of $1\frac{g}{L}$, and the sample is suspended in the fluid, firmly attached to a *Thorlabs* linear stage which allows fine adjustment of the height of 5 $\mu m$ per step. The travel of the linear stage is verified by a laser distance sensor with a range of 0.5 $mm$ and a resolution of 1 $\mu m$. The LED is powered at $2.8V$ and $0.7A$, and black cloth is placed over the setup to shield it from any ambient light. The camera was placed as close as possible while maintaining a sharp image at 20 $cm$ from the sample in order to maximise the resolution.

### B. Images

Images were taken at heights $0 - 100\ \mu m$ with $5 - 10\ \mu m$ steps, with fully opened aperture and an exposure time of $27,861\ ms$. For both samples, the $R_{h=0}$ image was taken at $0\ \mu m$. The camera sensor was used to separate the fluorescent light ($\lambda_{fl}$) from the incident light ($\lambda_i$), since the sensor sensitivity spectrum of red and green channels coincides with $\lambda_{fl}$ and $\lambda_i$ respectively.

Each image was cropped to center the sample in the frame and cropped further if air bubbles were present. Air bubbles on the sample greatly decrease the accuracy of this method, as they cause problems with determining the average intensity of the image and the creation of a smooth height map.

The image data is then filtered using a Gaussian blur. This blurring is done to average the intensity of multiple pixels to remove signal noise, which effectively trades spatial resolution with intensity accuracy. However, since the bearing surface is assumed smooth and deformable over the entire surface, this is not critical. The resulting image is then processed using equation 1. This results in a ratioed image which can be used to determine the fluid thickness if scaled correctly.

### C. Verification

Measurements from this method need to be verified with the use of an independent measurement method. This is done with the use of a *Bruker white light interferometer*, which can measure the height of the surface of the sample. It is able to stitch multiple measurements of a $2 \cdot 2\ mm$ area together to create a single image.

Five rows of 2 $mm$ wide are measured according to figure 3. Four surface measurements are taken 2 $mm$ from the respective edges. A fifth measurement is taken across the geometric centre of the sample. This data is then used to create a height map of sections of the samples, which is then compared to the corresponding data of the fluorescence test to validate the fluorescence test method. This is presented in figures 6a and 6b, with a detailed cross section view in figures 6c and 6d.

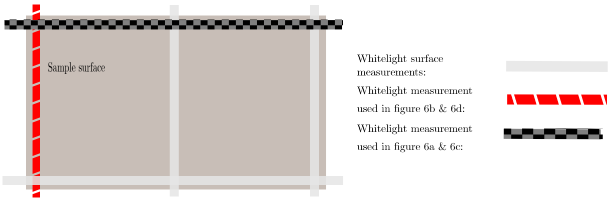


Fig. 3: Cross sections measured by white light interferometer

### D. Processing

The intensities of the images have to be processed in order to get a distributed film height measurement over the bearing surface.

First, the ratio values at each camera pixel are calculated using equation 1.

Then, the edge closest to the plate is determined. In the real application, this edge is assumed to be undeformed as there is no local film pressure pushing the bearing surface away from the running track [2].

The ratios along these edges are linearly scaled so that the average edge height of the minimum measurement matches 0 $\mu m$ and the average edge height of the maximum measurement matches 100 $\mu m$. This causes a deviation of the other measurements, which are depicted in figure 4.

Finally, $a$ is calculated by scaling the average height along these edges for each measurement, so that the height map of the image at 0 $\mu m$ corresponds to the undeformed bearing surface after using equation 2.

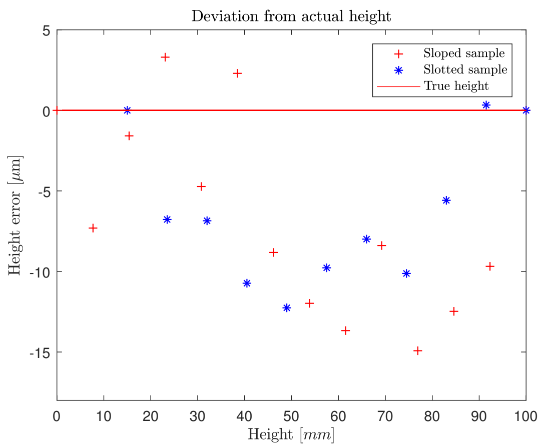


Fig. 4: Deviation from real height

The resulting surfaces are plotted against the white light interferometer data in figure 6c for the angled sample and in figure 6d for the slotted sample.

When these two results are combined a surface plot of the bearing on the correct height can be constructed.

## IV. Discussion

This method did not reach the same accuracy as the method it is adapted from. However, it serves as a proof of concept that it can be accurate enough to aid in the design of compliant hydrostatic bearings.

The large error in the measurement of the second sample as seen in figure 6a between $35-50$ $mm$ on the y axis is due to a reflection in the PMMA. Reflections in the PMMA are much brighter than the reflected light from the sample. The received data is not representative of the expected data and influences the measurements in a negative way. The slotted sample is only processed for half its length due to tiny air bubbles being present across its surface. These bubbles were found to have a large influence on the amount of reflected light. This distorted the data in such a way that the second half of the measurement became unusable.

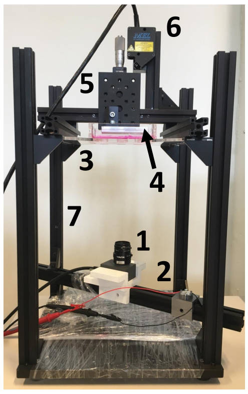


| no | Part |
|---|---|
| 1 | Camera: *Pixelink PL-D795* |
| 2 | LED: *LUXEON C - Mint* |
| 3 | PMMA tray |
| 4 | Sample |
| 5 | Linear stage: *Thorlabs* |
| 6 | Laser distance sensor: *M7L/0.5* |
| 7 | Frame: *Thorlabs optical rails* |

Fig. 5: Overview of test setup

Other sources of error might be caused due to insufficient distinction between $E_{\lambda_i}$ and $E_{\lambda_{fl}}$. The precision can therefore be improved by selecting a pigment with a larger Stokes shift, which results in less overlap between the absorption and emission spectra. Alternatively, a monochrome camera can be used with appropriately chosen optical band-pass filters. These can filter $E_{\lambda_i}$ and $E_{\lambda_{fl}}$ before the light reaches the camera, which eliminates the need for a colour sensor that has a certain sensitivity spectrum.

Another cause of error might be a difference in position and size of the white light measurements and the fluorescence measurements. These are effectively two matrices of different size and orientation, that need to be manually scaled and aligned. Accuracy can therefore be improved by optimizing this procedure or eliminating the need for it entirely.

Smaller height differences can be measured by using a camera with a higher radiometric resolution.

### *Conclusions*

A method to measure fluid thickness between a PMMA surface and a compliant hydrostatic bearing was developed. This method is able to create a height map of the bearing surface with an accuracy in the order of $10\mu m$. This method is able to measure total height with an accuracy of 15 $\mu m$. A method to calibrate and scale the surface measurements is presented. Real world applications will improve by differing LED and pigment combinations.

### *Recommendations*

*Rhodamine B* is toxic and not suited for a large scale test setup. Choosing a fluorescent pigment with a larger Stokes shift will ease the filtering of the incoming light. It is necessary to minimise the reflection of the PMMA plate. The precision of the measurement is dependant on the surface topography of the PMMA plate, so this must be verified. This method needs a uniform liquid layer to perform optimal, therefore it is necessary to minimise the amount of bubbles present on the measurement surface.

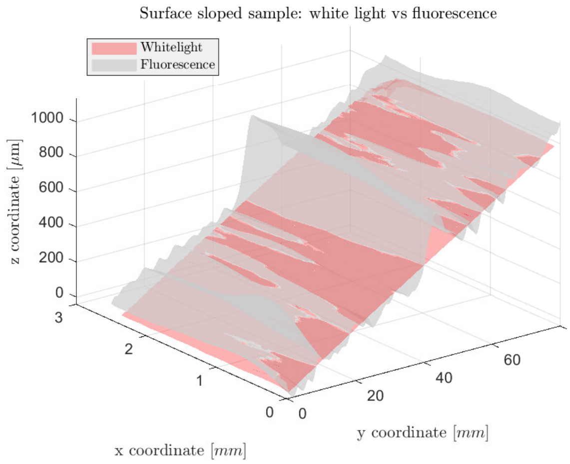


(a) Surface plot sloped sample

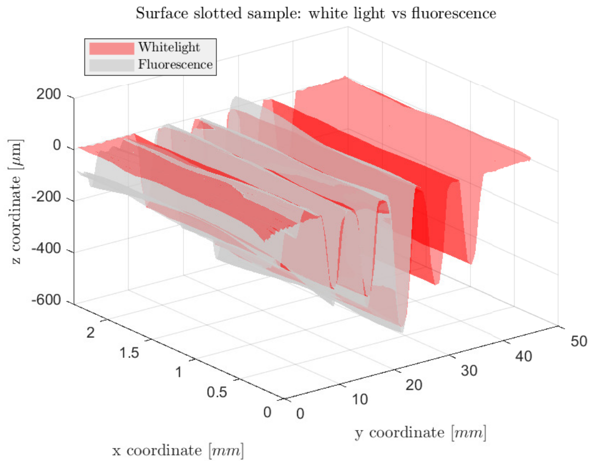


(b) Surface plot slotted sample

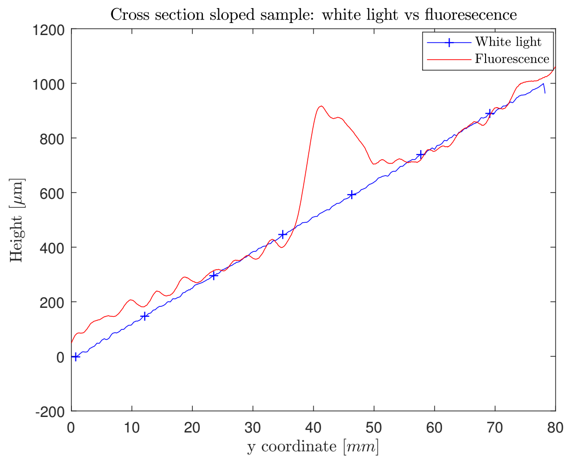


(c) Cross section sloped sample

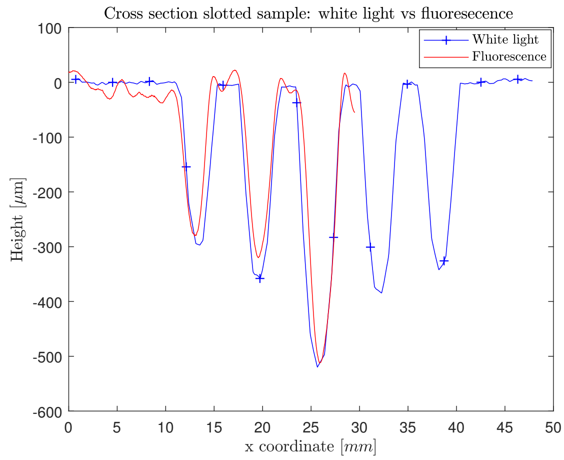


(d) Cross section slotted sample

Fig. 6: White light vs fluorescence

## REFERENCES


[1] K. L. Cavalca and H. I. Weber, Eds., *Proceedings of the 10th International Conference on Rotor Dynamics – IFToMM*. Springer International Publishing, 2019. [Online]. Available: https://doi.org/10.1007/978-3-319-99270-9

[2] R. Van Ostayen, "The hydro-support : An elasto-hydrostatic thrust bearing with mixed lubrication," Ph.D. dissertation, Delft University of Technology, 2002.

[3] J. Nijssen, N. Diepeveen, and A. Kempenaar, "Development of an interface between a plunger and an eccentric running track for a low-speed seawater pump," 06 2018.

[4] G. Sze-Wei, L. Han-Seok, M. Rahman, and F. Watt, "A fine tool servo system for global position error compensation for a miniature ultra-precision lathe," *International Journal of Machine Tools and Manufacture*, vol. 47, no. 7-8, pp. 1302–1310, 2007.

[5] T. Osman, M. Dorid, Z. Safar, and M. Mokhtar, "Experimental assessment of hydrostatic thrust bearing performance," *Tribology international*, vol. 29, no. 3, pp. 233–239, 1996.

[6] A. Mouza, N. Vlachos, S. Paras, and A. Karabelas, "Measurement of liquid film thickness using a laser light absorption method," *Experiments in Fluids*, vol. 28, pp. 355–359, 04 2000.

[7] R. Dwyer-Joyce, B. Drinkwater, and C. Donohoe, "The measurement of lubricant–film thickness using ultrasound," *Proceedings of the Royal Society of London. Series A: Mathematical, Physical and Engineering Sciences*, vol. 459, no. 2032, pp. 957–976, 2003.

[8] R. Bakke and P. Olsson, "Biofilm thickness measurements by light microscopy," *Journal of Microbiological Methods*, vol. 5, no. 2, pp. 93–98, 1986.

[9] T. A. Shedd and T. Newell, "Automated optical liquid film thickness measurement method," *Review of Scientific Instruments*, vol. 69, no. 12, pp. 4205–4213, 1998.

[10] L. Gustafsson, E. Höglund, and O. Marklund, "Measuring lubricant film thickness with image analysis," *Proceedings of the Institution of Mechanical Engineers, Part J: Journal of Engineering Tribology*, vol. 208, no. 3, pp. 199–205, 1994.

[11] G. Johnston, R. Wayte, and H. Spikes, "The measurement and study of very thin lubricant films in concentrated contacts," *Tribology Transactions*, vol. 34, no. 2, pp. 187–194, 1991.

[12] A. M. Khalil, "Two-dimensional displacement measurement using static close range photogrammetry and a single fixed camera," *Alexandria Engineering Journal*, vol. 50, no. 3, pp. 219–227, 2011.

[13] N. M. Husen, T. Liu, and J. P. Sullivan, "The ratioed image film thickness meter," *Measurement Science and Technology*, vol. 29, no. 6, p. 065301, 2018.

[14] M. Johnson, R. Schluter, and S. Bankoff, "Fluorescent imaging system for global measurement of liquid film thickness and dynamic contact angle in free surface flows," *Review of scientific instruments*, vol. 68, no. 11, pp. 4097–4102, 1997.

[15] C. Cenedese and S. Dalziel, "Concentration and depth fields determined by the light transmitted through a dyed solution," in *Proceedings of the 8th International Symposium on Flow Visualization*, vol. 8, 1998, pp. 1–37.

[16] Sigma-Aldrich, *Rhodamine B 95% (HPLC)*, 2019 (accessed June 5, 2019). [Online]. Available: https://www.sigmaaldrich.com/catalog/product/sigma/r6626?lang=en&region=NL

[17] OMLC, *Rhodamine B*, 2017 (accessed June 5, 2019). [Online]. Available: https://omlc.org/spectra/PhotochemCAD/html/009.html

[18] N. K. M. N. Srinivas, S. V. Rao, and D. N. Rao, "Saturable and reverse saturable absorption of rhodamine b in methanol and water," *J. Opt. Soc. Am. B*, vol. 20, no. 12, pp. 2470–2479, Dec 2003. [Online]. Available: http://josab.osa.org/abstract.cfm?URI=josab-20-12-2470

[19] E. Lepore, S. Brianza, F. Antoniolli, M. Buono, A. Carpinteri, and N. Pugno, "Preliminary in vivo experiments on adhesion of geckos," *Journal of Nanomaterials*, vol. 2008, 2008.